Received: 9 May 2022 | Revised: 11 July 2022 | Accepted: 7 August 2022

DOI: 10.1002/aic.17858

AIChE JOURNAL

RESEARCH ARTICLE

Biomolecular Engineering, Bioengineering, Biochemicals, Biofuels, and Food

Low dose chemotherapy induces a dormant state in brain metastatic breast cancer spheroids

Raghu Vamsi Kondapaneni | Rachel Warren | Shreyas S. Rao

Department of Chemical and Biological Engineering, The University of Alabama, Tuscaloosa, Alabama, USA

Correspondence
Shreyas S. Rao, Department of Chemical and Biological Engineering, The University of Alabama, Tuscaloosa, AL 35487-0203, USA.
Email: srao3@eng.ua.edu

Funding information
American Cancer Society, Grant/Award Number: RSG-21-032-01-CSM; METAvivor; National Science Foundation, Grant/Award Number: 1749837

Abstract

Surviving breast cancer cells post chemotherapy, metastasize, and develop recurrent tumors at distant organs. These cells are known to exhibit a dormant phenotype at metastatic sites and survive for extended periods of time. The mechanisms involved in attaining dormancy are unclear, including how chemotherapeutic drugs influence this state. Herein, we investigated the impact of a chemotherapy drug, paclitaxel, on brain metastatic breast cancer spheroids by culturing them in different drug concentrations for a period of 7 days. Our results demonstrated that spheroids survive lower doses (80 nM) of chemotherapy by exhibiting a dormant state and low levels of proliferation as characterized via Ki67 and EdU staining, as well as p-p38 and p-ERK, known markers of dormancy and proliferation. Upon withdrawal of drug, dormant spheroids attained growth indicating that the observed dormant state was reversible. Overall, these results provide insight into regulation of the dormant state mediated via low dose chemotherapy.

KEYWORDS
breast cancer, chemotherapy, dormancy, paclitaxel, spheroids

1 | INTRODUCTION

Breast cancer is the most often diagnosed cancer in women with over 300,000 new cases being recorded every year in the United States alone.[1] Over the past two decades, with major developments in early detection and therapeutic approaches, the mortality rate related to primary breast cancer has decreased significantly.[2] However, breast cancer is still responsible for the second most cancer related fatalities, because of its ability to metastasize and establish incurable recurrent tumors in multiple organs.[3] Recurrent tumors arising from breast cancer are frequently observed in the brain, lungs, liver, bones, and lymph node.[4] The time frame for these recurrent tumors, however, vary drastically from patient to patient, indicating a latency period wherein cancer cells survive for extended periods of time at a metastatic site by entering a dormant state.[3,5] Several key factors present in the secondary tumor microenvironment are known to aid these disseminated tumor cells (DTCs) in attaining a dormant state at the metastatic site.[5]

While surviving in a dormant state, metastatic tumor cells are known to develop resistance to therapies, as most therapies generally target proliferating tumor cells.[6,7] Specifically, DTCs are known to acquire chemotherapeutic resistance by upregulating the efflux transporter genes.[8] Accumulating evidence also suggests that stress signaling activated by chemotherapeutic drugs may induce a dormant state in metastatic tumors or DTCs.[9,10] Owing to the heterogeneity of solid tumors, lower doses of chemotherapeutic drugs reach the tumor site than the dose administered.[11] Zaleskis et al., reported that similar doses of chemotherapeutic drug (doxorubicin) administered in tumor bearing mice resulted in three different responses (cure, resistance, and relapse),[12] explaining the important role of heterogeneous cell populations. Chemotherapy drugs are also known to be present in the associated tissue for longer periods of time.[13] Thus, chemotherapeutic drugs significantly impact the regulation of metastatic dormancy and relapse.

The impact of chemotherapy drugs on breast tumor dormancy has been studied in both in vivo and in vitro settings.[5,14–20] For

instance, Lan et al., illustrated that ER$^-$ breast cancer cells survive higher doses of chemotherapy (doxorubicin and methotrexate) and exhibit dormancy in a mouse model by activating the IRF7/IFN-β/IFNAR axis.[18] Further, Tonnessen-Murray et al., elucidated that doxorubicin induced senescent cells exhibit a dormant like state by engulfing other cells.[15] Li et al., showed that breast and prostate cancer cells can attain a dormant state upon treatment with doxorubicin and docetaxel.[16] Clark et al., demonstrated that doxorubicin can eliminate only the proliferating cell population in an ex vivo model mimicking a hepatic niche, whereas dormant cell populations can survive and relapse.[17] Demicheli et al., reported that adjuvant chemotherapy in breast cancer patients was able to restrict the immediate and intermediate recurrent tumors, but not the long term recurrences.[19] However, to the best of our knowledge, the impact of chemotherapy on the regulation of dormancy in brain metastatic breast cancer (BMBC) has not been investigated.

Herein, we report the impact of low dose chemotherapy on modulating the dormant state in BMBC spheroids in vitro. We utilized paclitaxel as it is a commonly employed chemotherapeutic drug for metastatic breast cancer.[21] Three dimensional cell spheroids were employed as they closely mimic in vivo characteristics of cell clusters and/or micrometastasis (size of ∼200–2000 μm).[22] To prepare spheroids, we utilized 10,000 BMBC cells. Cell spheroids were cultured in drug containing media (0–100 μM) for 7 days in a poly(2-hydroxyethyl methacrylate) (p-HEMA) coated 96 well flat plate. Proliferating and dead cells present in spheroids were characterized to examine the impact of drug treatment. We also quantified the percentage of cells positive for phosphorylated extracellular regulated kinase 1/2 (p-ERK) and p-p38. Finally, we tested the reversibility of drug induced dormant state.

2 | MATERIALS AND METHODS

2.1 | Cell culture and paclitaxel dilutions

The td-Tomato expressing brain metastatic breast cancer cell line, MDA-MB-231Br (generously provided by Dr. Lonnie Shea, University of Michigan) was utilized in this study. These cells were cultured in T25 flasks in the presence of Dulbecco's Modified Eagle's Medium (Sigma Aldrich) containing 10% fetal bovine serum (VWR) and 1% penicillin streptomycin (Gibco) in a 37°C and 5% CO_2 environment. Upon reaching 80% confluency, cells were passaged using trypsin (Gibco). Cells below 30 passages were used for this study. Paclitaxel was procured from Sigma and diluted in the presence of DMSO to attain a stock concentration of 10 mM and further dilutions were prepared from this stock solution.

2.2 | Spheroid formation and culture

Spheroids were prepared as described previously.[23,24] Briefly, cell dilutions were prepared (10,000 cells/100 μl) and added to each well of a p-HEMA (Sigma Aldrich) coated 96 well conical bottom plate (Thermo Fisher) and centrifuged at 1000*g* for 10 min. Later, 2.5 μl of GFR Matrigel was added to each well and incubated overnight. On the next day, spheroids were transferred and cultured in a p-HEMA coated 96 well flat bottom plate in the presence of paclitaxel (Sigma Aldrich) containing media for 7 days. For every 2 days, 50 μl of drug containing media was added to each well. Images were taken every alternate day starting from day 1. Image J was used to calculate spheroid cross-sectional area and assess growth patterns. At the end of day 7, spheroids were dissociated into single cells for cell assays following a previously reported protocol.[23]

2.3 | Cell viability and nuclear green DCS1 assay

To detect cell viability and percentage of dead cells in spheroids, we performed Calcein AM (LIVE/DEAD™ Viability/Cytotoxicity Kit [Thermo Fisher Scientific]) and Nuclear green DCS1 (ab138905) staining as per manufacturer's protocol. For cell viability, on day 7, spheroids were incubated in 100 μl of fresh media containing 4 μM Calcein AM for 1 h in a 37°C and 5% CO_2 environment. Later, spheroids were washed in phosphate buffer saline (PBS) (Gibco) and imaged. For quantifying dead cells, spheroids were incubated overnight in the presence of 2 μM nuclear green DCS1 dye on day 6. On the following day, spheroids were washed twice with PBS and dissociated into single cells and imaged. An Olympus IX83 microscope with a spinning disk confocal attachment was utilized to capture fluorescence images and Image J was employed to quantify the percentage of dead cells.

2.4 | 5-Ethynyl-2′-deoxyuridine cell proliferation assay

5-Ethynyl-2′-deoxyuridine (EdU) (Click-iT™ EdU Cell Proliferation Kit [Thermo Fisher Scientific]) incorporation into cell DNA technique was employed to quantify proliferating cells as previously described.[23,25,26] Briefly, 10 μM EdU containing fresh drug media (100 μl) was added to each well by removing old drug media on day 6 and incubated overnight. On day 7, depending on the culture condition, spheroids were pooled together into a centrifuge tube, and washed twice with PBS and dissociated into single cells using accutase and added to a 96 well plate. Later, cells were fixed for 20 min at room temperature (RT), permeabilized for 15 min at RT, and blocked for 30 min at 4°C, as previously described.[23] Next, cells were incubated in EdU reaction cocktail for 30 min at RT in the dark. The reaction cocktail was prepared by following the manufacturer's protocol. Following this, cell nuclei were counter stained for DAPI (Invitrogen) for 5 min at RT in the dark. After each step, cells were washed with PBS and before aspirating any liquid from plate, the plate was centrifuged for 1 min to minimize cell loss. An Olympus IX83 microscope with a spinning disk confocal attachment was utilized to capture fluorescence images and Image J was employed to quantify the percentage of EdU positive cells.

2.5 | Immunofluorescence staining

Immunofluorescence staining was performed to detect Ki67, p-ERK, p-p38, and Cleaved caspase 3, which were differentially expressed between proliferating versus dormant spheroids as described in prior studies.[23,26,27] Briefly, on day 7, spheroids were dissociated into single cells and added to a 96 well plate. Single cells were fixed, permeabilized and blocked as described previously.[23] Later, cells were incubated in primary antibody (Ki67 [ab15580—1:150], cleaved caspase 3 [Asp175—1:200], p-ERK [C#4370S—1:200], p-p38 [C#922216S—1:200]) overnight at 4°C. On the following day, cells were incubated in secondary antibody (goat anti-rabbit antibody [A11034–1:1000, for Ki67, cleaved caspase 3, and p-ERK], goat anti-mouse antibody [A11001–1:1000, for p-p38]) to fluorescently label cells for 1 h at 4°C. Next, cell nuclei were counter stained for DAPI. After each step, cells were washed with PBS and before aspirating any liquid from plate, the plate was centrifuged for 1 min to minimize cell loss. Cells were imaged and quantified as mentioned above.

2.6 | Statistical analysis

A Student's *t*-test was performed to determine the *P*-values in JMP pro software. The data is reported as mean with standard error of the mean (SEM). The data set was considered to be statistically significant when the *P*-value was less than 0.05.

3 | RESULTS AND DISCUSSION

In this study, we characterized, for the first time, the impact of a chemotherapeutic drug, paclitaxel, on regulating dormancy in BMBC spheroids in vitro. Chemotherapeutic resistance is a major concern in breast cancer as well as other cancers.[21,28] Specifically, in the context of metastatic cancers, therapy resistant slow cycling cells are known to contribute to tumor relapse.[29,30] To eliminate dormant or drug resistant tumor cell populations, it is very critical to understand how drug treatments impact regulation of dormancy. Few studies have been reported to characterize the impact of chemotherapeutic drugs on tumor cell dormancy in vitro,[16,31] ex vivo,[17] and in vivo.[18,19,31–33] However, both the in vitro studies, investigated chemotherapeutic induced dormancy in single seeded breast[16] and colorectal[31] cancer cells cultured adherently in standard two dimensional tissue culture plates, which largely fail to mimic the key in vivo tumor characteristics. Herein, we utilized three dimensional spheroids as they are known to closely mimic in vivo tumor behaviors and are also utilized for screening drugs.[34,35]

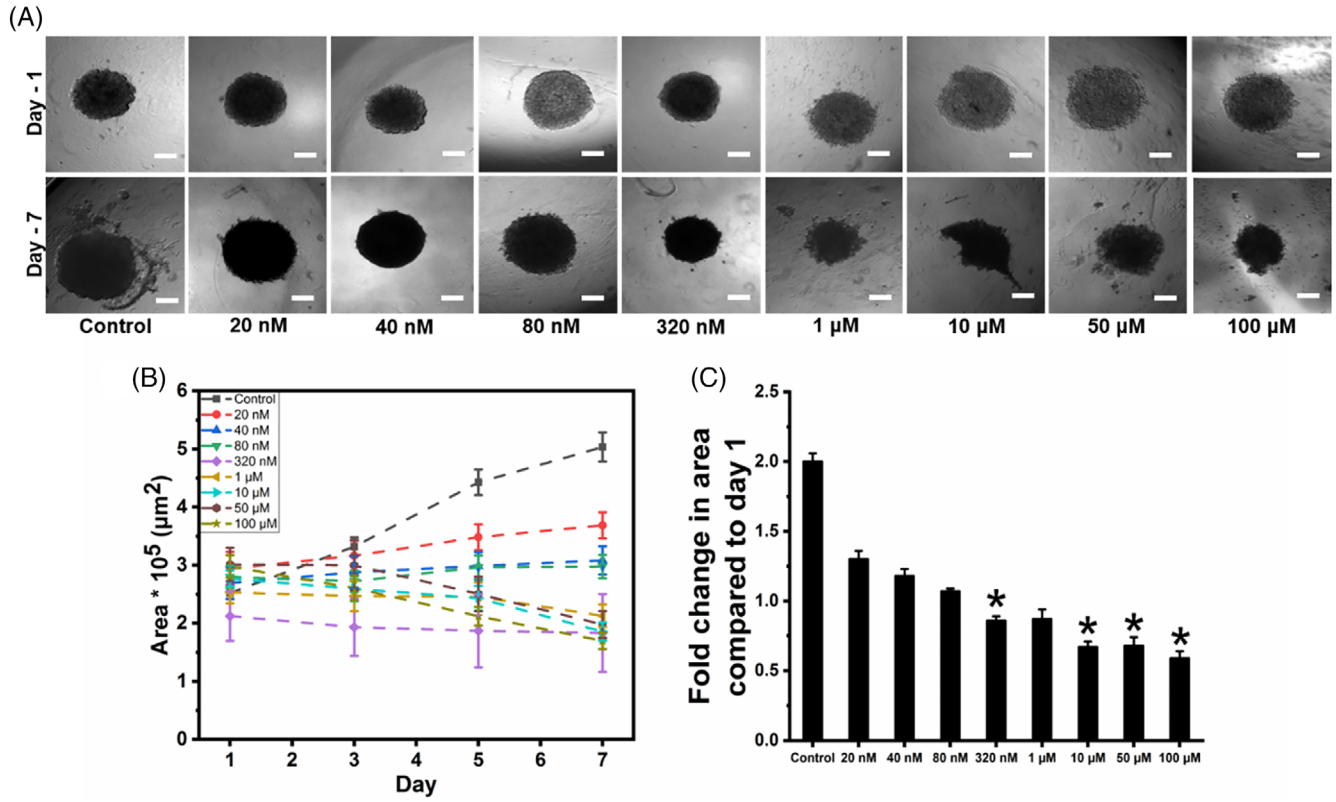

FIGURE 1 Cell spheroids exhibited differential growth responses depending on the paclitaxel concentration. (A) Day 1 and day 7 bright field images of untreated control spheroids, and those cultured in the presence of 20 nM, 40 nM, 80 nM, 320 nM, 1 μM, 10 μM, 50 μM, and 100 μM paclitaxel. Scale bar: 200 μm. (B) Cross sectional area of spheroids cultured in the presence of varying paclitaxel doses over a period of 7 days. (C) Day 7 fold change in area compared with day 1 for all drug doses. * indicates statistical significance ($P < 0.05$) for day 7 area compared with day 1 area. N ≥ 10 replicates for each condition.

3.1 | Cell spheroid growth and viability in the presence of paclitaxel

We cultured MDA-MB-231Br BMBC spheroids in the presence of paclitaxel for a period of 7 days in suspension culture, to investigate its impact on BMBC spheroid dormancy. We initially utilized eight drug concentrations ranging from 20 nM to 100 μM. Spheroids were also cultured without the presence of the drug, as a control. Cell spheroids were prepared by using 10,000 BMBC cells using a forced flotation on non-adhesive surfaces method.

Our results demonstrate that BMBC spheroids achieved growth in the absence of drug (day 1 area—243,703 ± 15,508 μm^2 vs. day 7 area—434,004 ± 31,119 μm^2), where the cross sectional area of the spheroid increased significantly from day 1 to day 7. Even in the presence of 20 and 40 nM drug concentrations an increase in cross sectional area was observed, however, this was

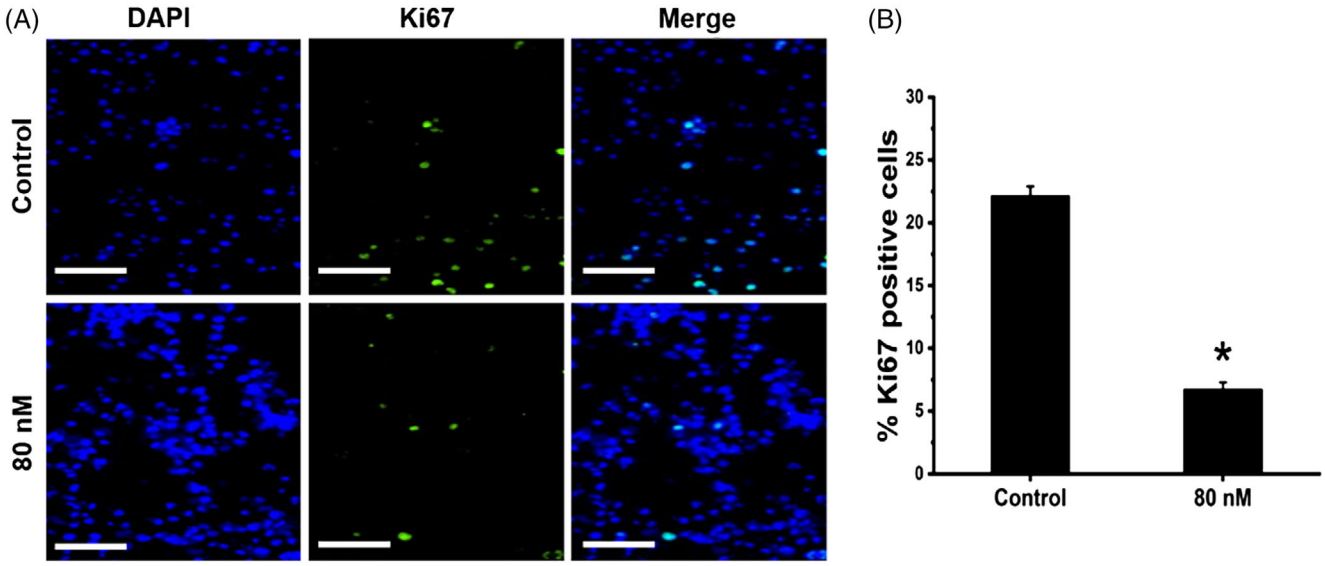

FIGURE 2 Cell spheroids displayed a dormant state with minimal cell proliferation when cultured in the presence of 80 nM paclitaxel. (A) Representative fluorescent images of Ki67 staining. (B) Quantification of % Ki67 positive cells. Scale bar: 100 μm. N ≥ 6 replicates for each condition. * indicates statistical significance ($P < 0.05$).

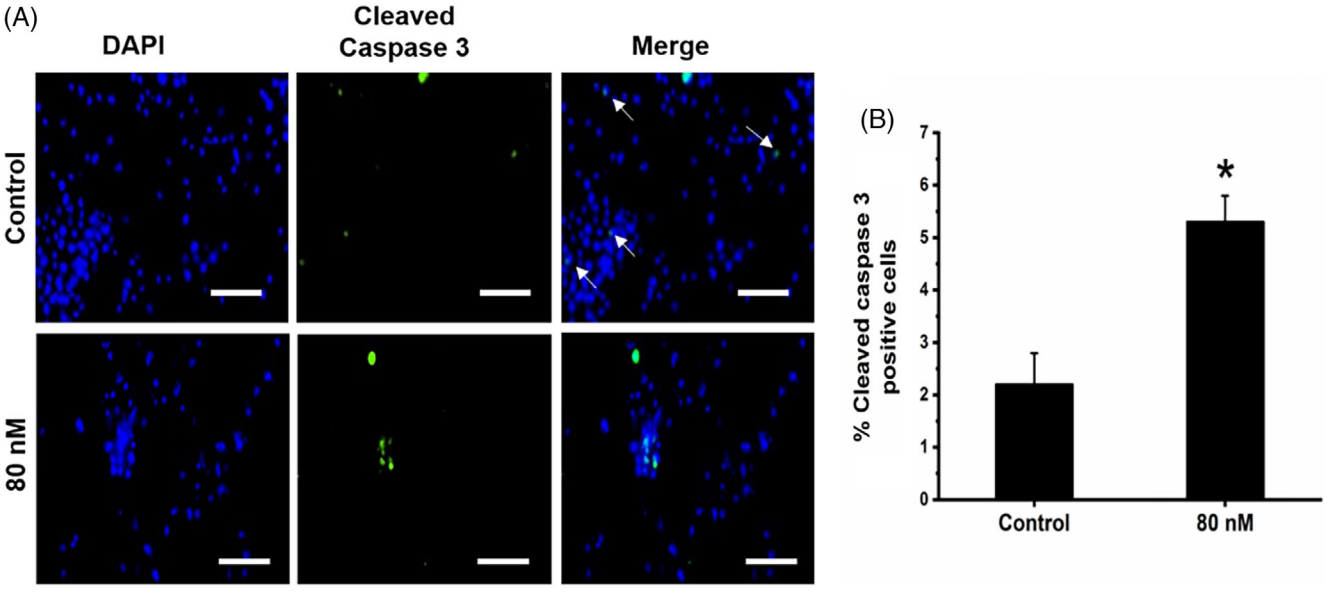

FIGURE 3 Percentage of apoptotic cells was higher in 80 nM drug treated spheroids compared with untreated control spheroids. (A) Representative fluorescent images of cleaved caspase 3 staining. (B) Quantification of % cleaved caspase 3 positive cells. Scale bar: 100 μm. N ≥ 6 replicates for each condition. * indicates statistical significance ($P < 0.05$).

not statistically significant (i.e., 20 nM [day 1 area—293,989 ± 29,028 μm^2 vs. day 7 area—368,693 ± 22,681 μm^2], 40 nM [day 1 area—269,231 ± 27,567 μm^2 vs. day 7 area—308,347 ± 24,326 μm^2]; Figure 1A,B). Interestingly, neither growth nor reduction in spheroid cross sectional area was observed in 80 nM concentration (day 1 area—279,799 ± 19,401 μm^2 vs. day 7 area—297,815 ± 20,259 μm^2), indicative of a quiescent or dormant state. However, with an increase in drug concentrations above 80 nM, a decrease in the cross-sectional area of spheroids was noted by the end of day 7 (Figure 1A,B). At higher concentrations (>200 nM), paclitaxel is known to kill cancer cells by inducing apoptosis,[36] which can be attributed to the decrease in cross-sectional area of spheroids cultured in higher concentrations of paclitaxel.

In addition to cross-sectional area measurements, we also calculated the fold change in area for day 7 compared with day 1, for all the drug concentrations (Figure 1C). In the untreated control condition, the fold change in area was 2.0 ± 0.06. For the various drug concentrations, day 7 fold change in area were as follows: 20 nM—1.3 ± 0.06, 40 nM—1.18 ± 0.05, 80 nM—1.07 ± 0.02, 320 nM—0.86 ± 0.03, 1 μM—0.87 ± 0.07, 10 μM—0.67 ± 0.04, 50 μM—0.68 ± 0.06, and 100 μM—0.59 ± 0.05. Previously, Mittler et al., reported similar observations in prostate cancer spheroids. Specifically, prostate cancer cell spheroid (VCaP and LNCaP) area was maintained constant for 4 days in the presence of lower concentrations (i.e., 50 nM) of the chemotherapy drug MLN4924.[37] In addition, drug dose dependent activation of dormant phenotype has been observed in mouse osteosarcoma and mammary sarcoma.[32,33] Here, we were able to establish

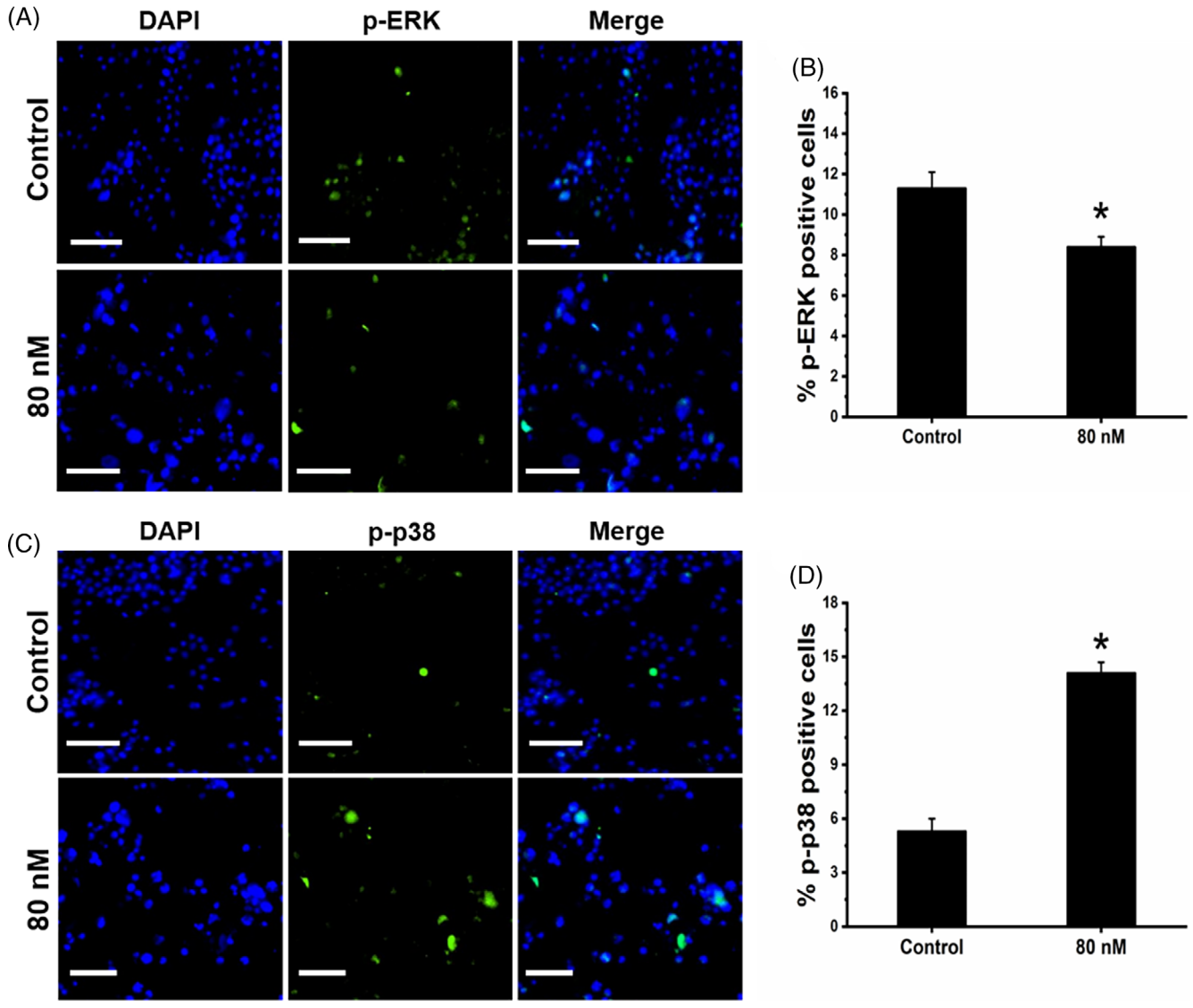

FIGURE 4 Percentage of p-p38 positive cells was higher while percentage of p-ERK positive cells was lower in 80 nM drug treated spheroids compared with untreated control spheroids. (A) Representative fluorescent images of p-ERK staining. (B) Quantification of % p-ERK positive cells. (C) Representative fluorescent images of p-p38 staining. (D) Quantification of % p-p38 positive cells. Scale bar: 100 μm. N ≥ 6 replicates for each condition. * indicates statistical significance ($P < 0.05$).

a concentration where no net growth was seen in MDA-MB-231Br BMBC spheroids. Thus, we utilized 80 nM paclitaxel treated spheroids for our subsequent studies, because the day 7 fold change in area compared with day 1 in this condition was nearly equal to 1 when compared with the 20 and 40 nM conditions.

Next, we investigated whether majority of cells present in 80 nM treated spheroid were viable by utilizing live/dead staining. As these MDA-MB-231Br cells already express red fluorescence we did not stain them for ethidium homodimer-1 (red dye) for dead cells. We stained both untreated control spheroids and 80 nM drug treated spheroids for Calcein AM to assess cell viability qualitatively. Calcein AM staining images depict that majority of cells were viable in both the conditions (Figure S1).

3.2 | Cell proliferation, death, p-ERK, and p-p38 positivity in BMBC spheroids

One of the main characteristics of a dormant state is the ability of cells to restrict their growth by arresting themselves in the G0/G1 phase.[3,5] To further characterize the observed dormant state in 80 nM drug treated cell spheroids, we measured the percentage of proliferating cells by detecting the Ki67 protein as well as by EdU incorporation. As expected, the percentage of proliferating cells were significantly higher in untreated controls compared with 80 nM drug treated spheroids. Specifically, untreated controls had 22.1% ± 0.8% Ki67 positive cells and 45.1% ± 2.1% EdU positive cells, respectively, whereas 80 nM drug treated spheroids had 6.7% ± 0.6% Ki67 positive cells and 21% ± 1.9% EdU positive cells, respectively (Figures 2 and S2). Previously, Li et al., demonstrated that SUM159 breast cancer cells cultured adherently on tissue culture plates upon treatment with docetaxel displayed a dormant phenotype with minimal cell proliferation compared with drug free cultures.[16] Our results are consistent with Li et al., and also demonstrate that such a state is achievable in BMBC spheroids.

Next, we quantified cell death in spheroids through the nuclear green DCS1 dye. Nuclear green DCS1 staining results demonstrated that 80 nM drug treated cell spheroids had a significantly higher percentage of dead cells (20.1% ± 2.6%) compared with untreated control spheroids (14.2% ± 1.2%; Figure S3). Even though a statistically significant difference was noted between both the conditions in the

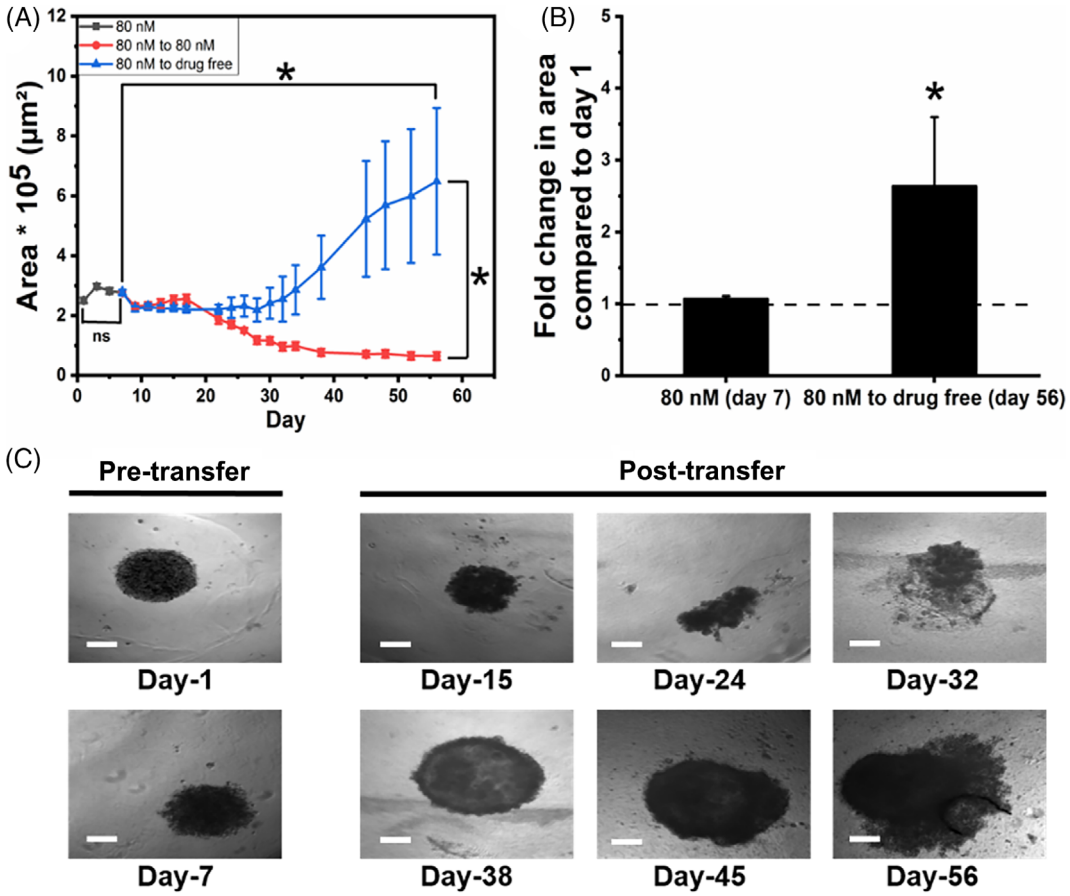

FIGURE 5 Dormancy induced in 80 nM drug treated spheroids was reversible. (A) Cross sectional area of spheroids cultured in the presence of 80 nM paclitaxel till day 7 and transferred and cultured in the presence of 80 nM paclitaxel or drug free media till day 56. (B) Day 7 fold change in area compared with day 1 for 80 nM (day 7) and 80 nM to drug free condition (day 56). (C) Bright field images of spheroids cultured in the presence of 80 nM paclitaxel (day 1 and 7) and in 80 nM to drug free condition (day 15, 24, 32, 38, 45, and 56). Scale bar: 200 µm. N ≥ 12 replicates for each condition. * indicates statistical significance ($P < 0.05$).

percentage of nuclear green DCS1 positive (dead) cells, more than 75% of cells were alive consistent with qualitative observations via Calcein AM staining (Figure S1). To quantify the percentage of apoptotic cells present in 80 nM drug treated and untreated control spheroids, we performed cleaved caspase 3 immunofluorescence staining. As paclitaxel is known to induce apoptosis,[38] apoptotic cell population was higher (5.3% ± 0.5%) in 80 nM treated spheroids compared with untreated control spheroids (2.2% ± 0.6%) (Figure 3). The rest of the cell death observed can be attributed to necrosis, which has been previously observed to occur in cell spheroids when the diameter is >400 μm.[39,40]

Previous studies have reported that in multiple cancers, tumor cells tend to achieve chemotherapeutic resistance by upregulating p-p38 expression.[41–44] In the context of dormancy, p-ERK/p-p38 activity ratio has been studied extensively, where lower activity ratio (<1) is indicative of the dormant state and high activity ratio is indicative of the proliferative state.[27,45,46] To identify if p-ERK and p-p38 are involved in attaining the dormant state in 80 nM drug treated spheroids, we performed p-ERK and p-p38 immunofluorescence staining. We found that the percentage of p-ERK positive cells were higher in untreated control spheroids, whereas percentage of p-p38 positive cells were higher in 80 nM drug treated spheroids. In particular, 80 nM drug treated spheroids had 14.1% ± 0.6% p-p38 positive cells and 8.4% ± 0.5% p-ERK positive cells. In contrast, untreated control spheroids had 5.3% ± 0.8% p-p38 positive cells and 11.8% ± 0.8% p-ERK positive cells (Figure 4). We also calculated the ratio of % p-ERK/%p-p38 positive cells. We observed that untreated control spheroids had a higher ratio of %p-ERK/%p-p38 positive cells (ratio ~ 2.2) compared with those in 80 nM drug treated spheroids (ratio ~ 0.6). These results indicated that 80 nM drug treated spheroids exhibited a dormant state by maintaining low levels of proliferation and an increase in percentage positivity for p-p38.

3.3 | Reversibility of paclitaxel induced dormancy in BMBC spheroids

Cells exhibiting dormancy can exit this state and develop aggressive tumors at later stages.[3,5,9,23] To this end, Li et al., previously

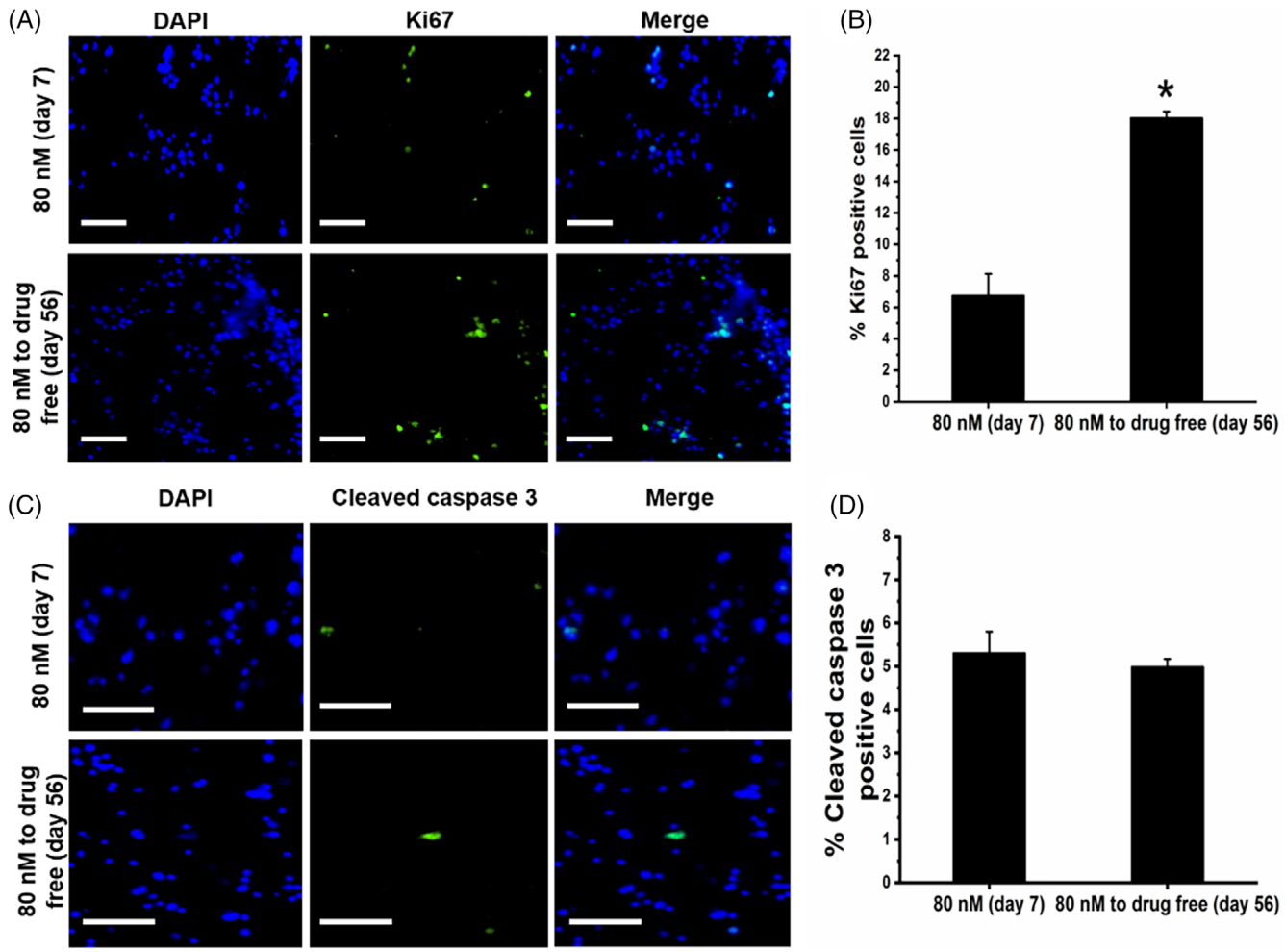

FIGURE 6 Cell spheroids exhibited a proliferative phenotype post-transfer to drug free media with an increase in percentage Ki67 positive cells on day 56. (A) Representative fluorescent images of Ki67 staining. (B) Quantification of % Ki67 positive cells. (C) Representative fluorescent images of cleaved caspase 3 staining. (D) Quantification of % cleaved caspase 3 positive cells. Scale bar: 100 μm. N ≥ 6 replicates for each condition. * indicates statistical significance ($P < 0.05$).

demonstrated that docetaxel induced dormancy in both breast and prostate cancer cells was reversed upon withdrawal of drug.[16] Here, to test whether the dormant state observed in 80 nM paclitaxel treated spheroids is reversible, we transferred the spheroids cultured in 80 nM drug containing media to drug free media. We also transferred and cultured spheroids in 80 nM drug containing media as a control. We found that growth was achieved in more than 80% of spheroids transferred from 80 nM drug containing media to drug free media (day 1 area—251,142 ± 8905 μm^2, day 7 area—272,343 ± 9663 μm^2, and day 56 area—649,193 ± 244,999 μm^2) by the end of day 56 (Figure 5A). For the initial 2 weeks post-transfer to drug free media, a slight decrease in spheroid cross-sectional area was noticed and interestingly spheroids exhibited irregular shapes until they started growing (Figure 5C). A continuous decline in spheroid cross-sectional areas was seen in the 80 nM to 80 nM condition (day 1 area—251,142 ± 8905 μm^2, day 7 area—272,343 ± 9663 μm^2, and day 56 area—65,099 ± 12,998 μm^2). We also calculated fold change in area which further confirmed that spheroids transferred from 80 nM drug containing media to drug free media attained growth (Figure 5B).

Next, we quantified the percentage of proliferating cells (% Ki67 positive cells) and apoptotic cells (% cleaved caspase 3 positive cells) in the 80 nM to drug free condition. The percentage of Ki67 positive cells in 80 nM to drug free condition on day 56 increased by three times compared with 80 nM drug treated spheroids on day 7. Specifically, 18% ± 0.4% Ki67 positive cells were present in 80 nM to drug free condition, whereas 6.7% ± 0.6% Ki67 positive cells were present in 80 nM treated spheroids (Figure 6A,B). No change in the percentage of apoptotic cells was observed in 80 nM to drug free condition (5.0% ± 0.2%) compared with 80 nM condition (5.3% ± 0.5%) (Figure 6C,D). This could be because lower concentrations of paclitaxel (10–100 nM) typically arrests cell growth rather than inducing apoptosis.[36] Collectively, these results suggest that chemotherapy induced dormant state is reversible upon withdrawal of the drug and can occur over longer time scales. Overall, our results provide an in vitro model to study chemotherapy drug induced dormancy in BMBC spheroids. In the future, we are planning to analyze the genes that are upregulated in the chemotherapy induced dormant state versus drug free proliferative state.

4 | CONCLUSIONS

We successfully developed an in vitro model demonstrating the impact of lower concentrations of chemotherapeutic drug paclitaxel on BMBC spheroid dormancy. Cell spheroids displayed a proliferative phenotype in the absence of the drug whereas dose dependent growth patterns were observed in the presence of varying drug doses. For doses <80 nM, spheroid cross-sectional area increased, and spheroid area decreased for doses >80 nM. Spheroids cultured in the presence of 80 nM paclitaxel exhibited a dormant state with low levels of proliferation as tested via Ki67 and EdU staining when compared with untreated control spheroids. The percentage of p-ERK positive cells decreased while the percentage of p-p38 positive cells increased in 80 nM paclitaxel treated spheroids compared with untreated control spheroids. Drug induced dormancy was reversed upon culturing the spheroids in absence of the drug. In summary, our results demonstrated that low dose chemotherapy can modulate the dormant state and these aspects must be considered in designing future therapeutic strategies.

AUTHOR CONTRIBUTIONS

Raghu Vamsi Kondapaneni: Conceptualization (equal); data curation (lead); formal analysis (lead); investigation (lead); methodology (equal); validation (lead); visualization (lead); writing – original draft (lead); writing – review and editing (equal). **Rachel Warren:** Data curation (supporting); formal analysis (supporting); investigation (supporting); methodology (supporting); validation (supporting); writing – original draft (supporting); writing – review and editing (equal). **Shreyas Rao:** Conceptualization (equal); funding acquisition (lead); methodology (equal); project administration (lead); resources (lead); supervision (lead); writing – review and editing (equal).

ACKNOWLEDGMENTS

This work was supported by the American Cancer Society (RSG-21-032-01-CSM), and, in part, by METAvivor, and the National Science Foundation (CBET 1749837).

CONFLICT OF INTEREST

The authors declare that there are no conflicts of interest.

DATA AVAILABILITY STATEMENT

The data that support the findings of this study are available from the corresponding author upon reasonable request.

ORCID

Shreyas S. Rao https://orcid.org/0000-0001-7649-0171

REFERENCES

1. Bushnell GG, Deshmukh AP, den Hollander P, et al. Breast cancer dormancy: need for clinically relevant models to address current gaps in knowledge. *NPJ Breast Cancer*. 2021;7(1):66.
2. Lim AR, Ghajar CM. Thorny ground, rocky soil: tissue-specific mechanisms of tumor dormancy and relapse. *Semin Cancer Biol*. 2022;78:104-123.
3. Rao SS, Kondapaneni RV, Narkhede AA. Bioengineered models to study tumor dormancy. *J Biol Eng*. 2019;13:3.
4. Jin X, Mu P. Targeting breast cancer metastasis. *Breast Cancer*. 2015;9:23-34.
5. Pradhan S, Sperduto JL, Farino CJ, Slater JH. Engineered in vitro models of tumor dormancy and reactivation. *J Biol Eng*. 2018;12(1):37.
6. Santos-de-Frutos K, Djouder N. When dormancy fuels tumour relapse. *Commun Biol*. 2021;4(1):747.
7. Park S-Y, Nam J-S. The force awakens: metastatic dormant cancer cells. *Exp Mol Med*. 2020;52(4):569-581.
8. Cao J, Zhang M, Wang B, Zhang L, Zhou F, Fang M. Chemoresistance and metastasis in breast cancer molecular mechanisms and novel clinical strategies. *Front Oncol*. 2021;11:658552.
9. Sosa MS, Bragado P, Aguirre-Ghiso JA. Mechanisms of disseminated cancer cell dormancy: an awakening field. *Nat Rev Cancer*. 2014;14(9):611-622.

10. Adam AP, George A, Schewe D, et al. Computational identification of a p38SAPK-regulated transcription factor network required for tumor cell quiescence. *Cancer Res*. 2009;69(14):5664-5672.
11. Hafeez MN, Celia C, Petrikaite V. Challenges towards targeted drug delivery in cancer nanomedicines. *Processes*. 2021;9(9):1527.
12. Zaleskis G, Garberytė S, Pavliukevičienė B, et al. Doxorubicin uptake in ascitic lymphoma model: resistance or curability is governed by tumor cell density and prolonged drug retention. *J Cancer*. 2020; 11(22):6497-6506.
13. Zaleskis G, Garberytė S, Pavliukevičienė B, et al. A model of chemotherapy-induced tumor dormancy: doxorubicin retention and degradation defines resumed growth in vivo; 2021.
14. Imamura Y, Mukohara T, Shimono Y, et al. Comparison of 2D- and 3D-culture models as drug-testing platforms in breast cancer. *Oncol Rep*. 2015;33(4):1837-1843.
15. Tonnessen-Murray CA, Frey WD, Rao SG, et al. Chemotherapy-induced senescent cancer cells engulf other cells to enhance their survival. *J Cell Biol*. 2019;218(11):3827-3844.
16. Li S, Kennedy M, Payne S, et al. Model of tumor dormancy/recurrence after short-term chemotherapy. *PLoS One*. 2014;9(5): e98021.
17. Clark AM, Kumar MP, Wheeler SE, et al. A model of dormant-emergent metastatic breast cancer progression enabling exploration of biomarker signatures. *Mol Cell Proteom*. 2018;17(4):619-630.
18. Lan Q, Peyvandi S, Duffey N, et al. Type I interferon/IRF7 axis instigates chemotherapy-induced immunological dormancy in breast cancer. *Oncogene*. 2019;38(15):2814-2829.
19. Demicheli R, Desmedt C, Retsky M, Sotiriou C, Piccart M, Biganzoli E. Late effects of adjuvant chemotherapy adumbrate dormancy complexity in breast cancer. *Breast*. 2020;52:64-70.
20. Demicheli R, Miceli R, Moliterni A, et al. Breast cancer recurrence dynamics following adjuvant CMF is consistent with tumor dormancy and mastectomy-driven acceleration of the metastatic process. *Ann Oncol*. 2005;16(9):1449-1457.
21. Rivera E, Gomez H. Chemotherapy resistance in metastatic breast cancer: the evolving role of ixabepilone. *Breast Cancer Res*. 2010; 12(2):S2.
22. Sahin AA, Guray M, Hunt KK. Identification and biologic significance of micrometastases in axillary lymph nodes in patients with invasive breast cancer. *Arch Pathol Lab Med*. 2009;133(6):869-878.
23. Kondapaneni RV, Rao SS. Matrix stiffness and cluster size collectively regulate dormancy versus proliferation in brain metastatic breast cancer cell clusters. *Biomater Sci*. 2020;8(23):6637-6646.
24. Ivascu A, Kubbies M. Rapid generation of single-tumor spheroids for high-throughput cell function and toxicity analysis. *J Biomol Screen*. 2006;11(8):922-932.
25. Nakod PS, Kim Y, Rao SS. Three-dimensional biomimetic hyaluronic acid hydrogels to investigate glioblastoma stem cell behaviors. *Biotechnol Bioeng*. 2020;117(2):511-522.
26. Narkhede AA, Crenshaw JH, Crossman DK, Shevde LA, Rao SS. An in vitro hyaluronic acid hydrogel based platform to model dormancy in brain metastatic breast cancer cells. *Acta Biomater*. 2020;107: 65-77.
27. Farino Reyes CJ, Pradhan S, Slater JH. The influence of ligand density and degradability on hydrogel induced breast cancer dormancy and reactivation. *Adv Healthc Mater*. 2021;10(11):2002227.
28. Alfarouk KO, Stock C-M, Taylor S, et al. Resistance to cancer chemotherapy: failure in drug response from ADME to P-gp. *Cancer Cell Int*. 2015;15:71.
29. Moore N, Houghton J, Lyle S. Slow-cycling therapy-resistant cancer cells. *Stem Cells Dev*. 2012;21(10):1822-1830.
30. Basu S, Dong Y, Kumar R, Jeter C, Tang DG. Slow-cycling (dormant) cancer cells in therapy resistance, cancer relapse and metastasis. *Semin Cancer Biol*. 2022;78:90-103.
31. Wu F-H, Mu L, Li X-L, et al. Characterization and functional analysis of a slow-cycling subpopulation in colorectal cancer enriched by cell cycle inducer combined chemotherapy. *Oncotarget*. 2017;8(45): 78466-78479.
32. Tomoda R, Seto M, Hioki Y, et al. Low-dose methotrexate inhibits lung metastasis and lengthens survival in rat osteosarcoma. *Clin Exp Metastasis*. 2005;22(7):559-564.
33. Aqbi H, Coleman C, Idowu M, Manjili M. Low-dose chemotherapy induces immunogenic tumor dormancy in mouse mammary carcinoma cells. *J Immunol*. 2019;202:194-197.
34. Zanoni M, Piccinini F, Arienti C, et al. 3D tumor spheroid models for in vitro therapeutic screening: a systematic approach to enhance the biological relevance of data obtained. *Sci Rep*. 2016;6(1):19103.
35. Nunes AS, Barros AS, Costa EC, Moreira AF, Correia IJ. 3D tumor spheroids as in vitro models to mimic in vivo human solid tumors resistance to therapeutic drugs. *Biotechnol Bioeng*. 2019;116(1): 206-226.
36. Wang TH, Wang HS, Soong YK. Paclitaxel-induced cell death: where the cell cycle and apoptosis come together. *Cancer*. 2000;88(11): 2619-2628.
37. Mittler F, Obeïd P, Rulina AV, Haguet V, Gidrol X, Balakirev MY. High-content monitoring of drug effects in a 3D spheroid model. *Front Oncol*. 2017;7:293.
38. Yeung TK, Germond C, Chen X, Wang Z. The mode of action of taxol: apoptosis at low concentration and necrosis at high concentration. *Biochem Biophys Res Commun*. 1999;263(2):398-404.
39. Singh M, Mukundan S, Jaramillo M, Oesterreich S, Sant S. Three-dimensional breast cancer models mimic hallmarks of size-induced tumor progression. *Cancer Res*. 2016;76(13):3732-3743.
40. Kunz-Schughart LA, Freyer JP, Hofstaedter F, Ebner R. The use of 3-D cultures for high-throughput screening: the multicellular spheroid model. *J Biomol Screen*. 2004;9(4):273-285.
41. García-Cano J, Roche O, Cimas FJ, et al. p38MAPK and chemotherapy: we always need to hear both sides of the story. *Front Cell Dev Biol*. 2016;4:69.
42. Guo X, Ma N, Wang J, et al. Increased p38-MAPK is responsible for chemotherapy resistance in human gastric cancer cells. *BMC Cancer*. 2008;8:375.
43. Losa JH, Cobo CP, Viniegra JG, Lobo VJS-A, Cajal SRY, Sánchez-Prieto R. Role of the p38 MAPK pathway in cisplatin-based therapy. *Oncogene*. 2003;22(26):3998-4006.
44. Donnelly SM, Paplomata E, Peake BM, Sanabria E, Chen Z, Nahta R. P38 MAPK contributes to resistance and invasiveness of HER2- overexpressing breast cancer. *Curr Med Chem*. 2014;21(4):501-510.
45. Aguirre-Ghiso JA, Estrada Y, Liu D, Ossowski L. ERKMAPK activity as a determinant of tumor growth and dormancy; regulation by p38SAPK1. *Cancer Res*. 2003;63(7):1684-1695.
46. Ranganathan AC, Adam AP, Zhang L, Aguirre-Ghiso JA. Tumor cell dormancy induced by p38SAPK and ER-stress signaling: an adaptive advantage for metastatic cells? *Cancer Biol Ther*. 2006;5(7):729-735.

SUPPORTING INFORMATION

Additional supporting information can be found online in the Supporting Information section at the end of this article.

How to cite this article: Kondapaneni RV, Warren R, Rao SS. Low dose chemotherapy induces a dormant state in brain metastatic breast cancer spheroids. *AIChE J*. 2022;68(12): e17858. doi:10.1002/aic.17858